Viscoelastic properties of tumor spheroids revealed by a microfluidic compression device and a modified power law model

Mrinal Pandey[1], Bangguo Zhu[3], Kaitlyn Roach[2], Young Joon Suh[1], Jeffrey E Segall[4], Chung-Yuen Hui[3], and Mingming Wu[1]

[1]Biological and Environmental Engineering Department, Cornell University, Ithaca, NY, USA

[2] Meinig School of Biomedical Engineering, Cornell University, Ithaca, NY. USA.

[3]Sibley School of Mechanical and Aerospace Engineering, Cornell University, Ithaca, NY. USA.

[4]Department of Pathology, Albert Einstein College of Medicine, 1300 Morris Park Avenue, Bronx, NY, USA 10461

Supplementary materials

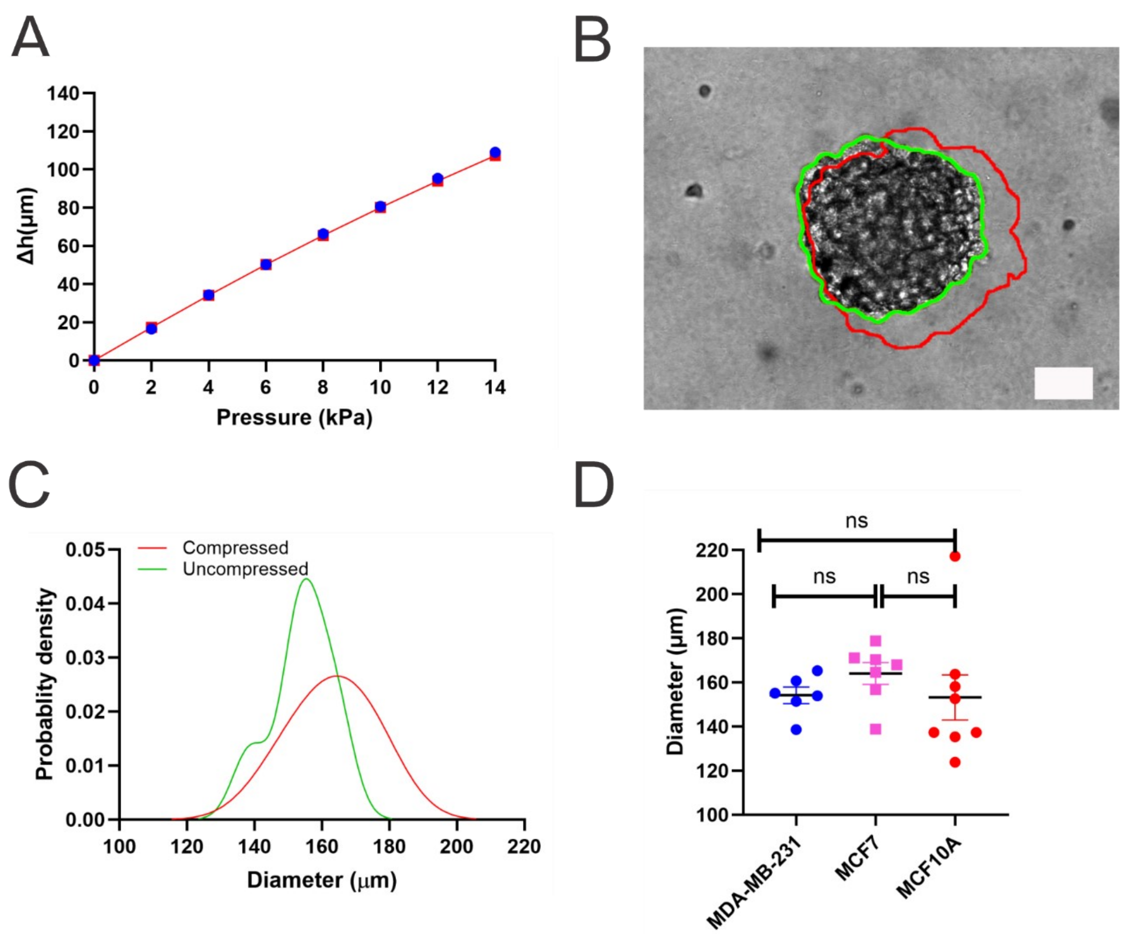

Figure S1: (A) Device calibration. Deflection of the piston as a function of pressure applied (dots are experiments and the red line is COMSOL computation result). **(B)** A bright field image of MDA-MB-231 spheroid embedded in collagen. The red or green outline marks the peripheral of the spheroid with and without compression respectively. The compression pressure is 14 kPa. The scale bar is 50 µm. (**C**) Size distribution of MDA-MB-231 spheroids before and after compression. **(D)** Measured diameter of spheroids made of three different breast cell lines with increasing malignancy before compression: non-tumorigenic MCF10A, ER positive tumorigenic MCF7 and triple negative metastatic MDA-MB-231. The significance data is obtained using a nonparametric t-test (Mann–Whitney test).

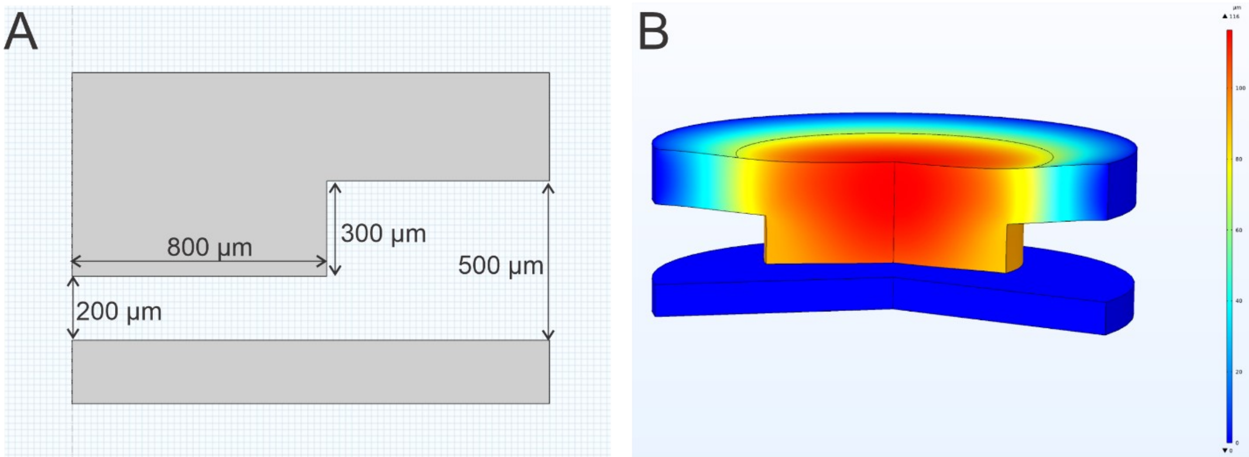

Figure S2: (A) Dimensions of a compression unit. (B) COMSOL simulation of vertical displacement of deformable piston layer upon application of 14 kPa pressure.

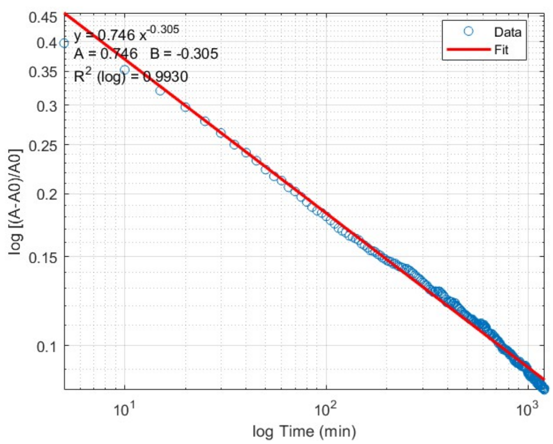

Figure S3: Log-log plot for MCF10A spheroid relaxation area upon load removal. The relaxation time is 20 minutes. Blue circles are from the experiment, and the red line is a power law fit.

Theoretical models:

1. **Modified Power law model to fit tumor spheroid compression data**

The relaxation function of the modified power-law model is given by[1],

$$Y(t) = E_\infty + \frac{E_0 - E_\infty}{\left(1 + \frac{t}{t_R}\right)^m} \#(S1)$$

where $E_0 = Y(t = 0)$ is the instantaneous Young's modulus, $E_\infty = Y(t \to +\infty)$ is the relaxation Young's modulus or long-time modulus, t_R and m are two material fitting parameters. The modulus smoothly decreases from E_0 to E_∞ with increasing time. Here, we define the ratio of instantaneous modulus and relaxation modulus as $\rho = E_0/E_\infty > 1$

An approximate expression for the corresponding creep function $C(t)$ associated with this $Y(t)$ is given in [2]

$$C(t) \approx \frac{Y(t)}{Y^2(t) + \left(\frac{\pi t}{2}\right)^2 \left[\frac{d\,Y(t)}{d\,t}\right]^2} \#(S2)$$

Substituting Eq. (S3) into Eq. (S4),

$$C(t) \approx \frac{E_\infty + \frac{E_0 - E_\infty}{\left(1 + \frac{t}{t_R}\right)^m}}{\left[E_\infty + \frac{E_0 - E_\infty}{\left(1 + \frac{t}{t_R}\right)^m}\right]^2 + \left(\frac{m\pi t}{2t_R}\right)^2 \left[\frac{E_0 - E_\infty}{\left(1 + \frac{t}{t_R}\right)^{m+1}}\right]^2} \#(S3)$$

We approximate the deformation of the spheroid during one loading-unloading cycle by a 1D uniaxial linear viscoelastic model where the uniaxial strain ε is identified with $\Delta h/h$. The strain history is:

a. At $t = 0$, a sudden compression strain ε_0 is applied. Note in the following discussion, we take the absolute values of all compression strain, so all strains values are positive.

b. For $0 < t < T$, strain is held constant. The system is under stress relaxation. The stress in this stage is given by, $\sigma(t) = Y(t)\varepsilon_0$. [2].

c. At $t = T$, the system is suddenly unloaded. Stress drops to zero, $\sigma(t > T^+) = 0$, and strain starts to decrease in this strain recovery stage.

The stress history can be expressed with the help of Heaviside step function $H(x) = \begin{cases} 1, x \geq 0 \\ 0, x < 0 \end{cases}$,

$$\sigma = Y(t)\varepsilon_0[H(t) - H(t - T)] \#(S4)$$

The strain history from the Boltzmann superposition principle is,

$$\varepsilon(t) = \varepsilon_0 H(t) - \varepsilon_0 \int_0^t C(t-\tau) \frac{d[Y(\tau)H(\tau - T)]}{d\tau} d\tau \#(S5)$$

For $0 < t < T$, the integral in Eq.(S5) is zero and $\varepsilon(0 < t < T) = \varepsilon_0$.

For $t > T$, the Eq.(S5) leads to,

$$\varepsilon(t > T) = \varepsilon_0 - \varepsilon_0 \left[C(t-T)Y(T) + \int_{T^+}^t C(t-\tau) \frac{dY(\tau)}{d\tau} d\tau \right] \#(S6a)$$

$$\bar{\varepsilon}(t > T) \triangleq \frac{\varepsilon(t > T)}{\varepsilon_0} = 1 - \frac{\left[1 + \frac{\rho - 1}{\left(1 + \frac{t-T}{t_R}\right)^m}\right]\left[1 + \frac{\rho - 1}{\left(1 + \frac{T}{t_R}\right)^m}\right]}{\left[1 + \frac{\rho - 1}{\left(1 + \frac{t-T}{t_R}\right)^m}\right]^2 + \left[\frac{m\pi(t-T)}{2t_R}\right]^2 \left[\frac{\rho - 1}{\left(1 + \frac{t-T}{t_R}\right)^{m+1}}\right]^2}$$

$$+ \frac{m}{t_R} \int_{T^+}^t \frac{\left[1 + \frac{\rho - 1}{\left(1 + \frac{t-\tau}{t_R}\right)^m}\right]\left[\frac{\rho - 1}{\left(1 + \frac{\tau}{t_R}\right)^{m+1}}\right]}{\left[1 + \frac{\rho - 1}{\left(1 + \frac{t-\tau}{t_R}\right)^m}\right]^2 + \left[\frac{m\pi(t-\tau)}{2t_R}\right]^2 \left[\frac{\rho - 1}{\left(1 + \frac{t-\tau}{t_R}\right)^{m+1}}\right]^2} d\tau \#(S6b)$$

If we take the limit $t \to T^+$, we have the normalized strain at the instant after the sudden unloading given by,

$$\bar{\varepsilon}(T^+) = 1 - \frac{\left[1 + \frac{\rho - 1}{\left(1 + \frac{T}{t_R}\right)^m}\right]}{\rho} = 1 - \frac{1}{\rho} - \frac{\rho - 1}{\rho} \frac{1}{\left(1 + \frac{T}{t_R}\right)^m} \#(S7a)$$

which means the sudden strain drop at unloading $t = T$ is,

$$\varepsilon_{\text{drop}} = \left|\bar{\varepsilon}(T^+) - \bar{\varepsilon}(T^-)\right| = \left[\frac{1}{\rho} + \frac{\rho - 1}{\rho} \frac{1}{\left(1 + \frac{T}{t_R}\right)^m}\right] \#(S7b)$$

This 1D theory explains the sudden strain drop and subsequent creep observed in our experiments. Experimental data fitting using Eq.(S6b) and Eq.(S7b) suggests $\rho \gg 1$, likely due to active rearrangements in the living tumor spheroid, consistent with a fluid-like long-time response $(E_\infty \to 0)$.

Considering the time scale in our experiments, we can safely assume $E_\infty = 0, \rho \to +\infty$ in the above equations and take t_R, m as the only fitting parameters. In the $\rho \to +\infty$ limit, the normalized strain becomes,

$$\bar{\varepsilon}(t>T) = 1 - \frac{\left(1+\frac{t-T}{t_R}\right)^{m+2}}{\left(1+\frac{t-T}{t_R}\right)^2 + \left[\frac{m\pi(t-T)}{2t_R}\right]^2}\left[\frac{1}{\left(1+\frac{T}{t_R}\right)^m}\right]$$

$$+\frac{m}{t_R}\int_{T^+}^{t} \frac{\left(1+\frac{t-\tau}{t_R}\right)^{m+2}}{\left(1+\frac{t-\tau}{t_R}\right)^2 + \left[\frac{m\pi(t-\tau)}{2t_R}\right]^2}\left[\frac{1}{\left(1+\frac{\tau}{t_R}\right)^{m+1}}\right] d\tau \# (S8a)$$

$$\varepsilon_{\text{drop}} = \left|\bar{\varepsilon}(T^+) - \bar{\varepsilon}(T^-)\right| = \frac{1}{\left(1+\frac{T}{t_R}\right)^m} \# (S8b)$$

The Eq. (S8a, b) are used to obtain t_R, m from fitting the sudden drop of strain after unloading and the following gradual strain decreasing in the creeping stage.

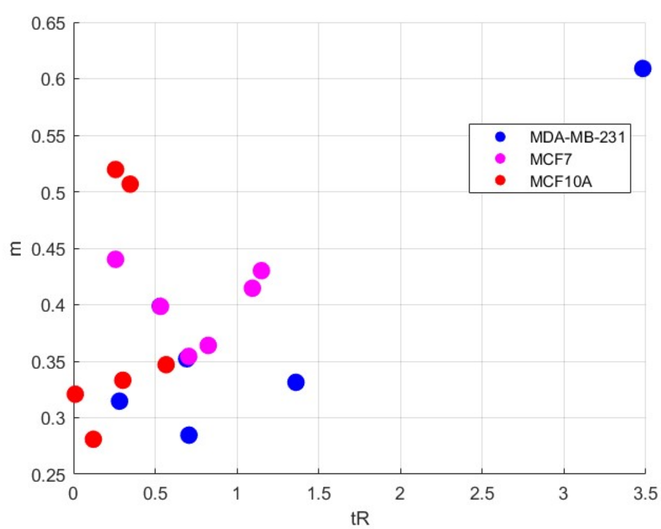

Figure S4: Fitted parameter values for m and t_R, values for spheroids made of three different cell types, very malignant (MDA-MB-231), moderately malignant (MCF7) and non-tumorigenic (MCF10A) breast tumor cells. Each dot fits the data of response curve of one spheroid. These values are obtained from 18 different spheroids with a total of 6 spheroids from each cell line.

2. **Effective viscosity calculation**

In linear viscoelastic theory, the energy dissipated per cycle under sinusoidal strain $\varepsilon(t) = \varepsilon_0 \cos \omega t$ is given by,

$$W_D = \varepsilon_0^2 \omega E^{''}(\omega) \int_0^{\frac{2\pi}{\omega}} \sin^2(\omega t) dt = \pi \varepsilon_0^2 \omega E^{''}(\omega) \# (S9)$$

If we assume that at any fixed frequency ω, the dissipation is due to a dashpot with viscosity $\eta(\omega)$, analogous to a Newtonian fluid,

$$\sigma = \eta(\omega)\dot{\varepsilon} \# (S10)$$

This leads to the energy dissipation per cycle,

$$W_D = \int_0^{\frac{2\pi}{\omega}} \sigma d\varepsilon = \int_0^{\frac{2\pi}{\omega}} \eta(\omega)\dot{\varepsilon} d\varepsilon = - \varepsilon_0 \omega \eta(\omega) \int_0^{\frac{2\pi}{\omega}} \sin(\omega t) d\varepsilon$$

$$= \varepsilon_0^2 \omega^2 \eta(\omega) \int_0^{\frac{2\pi}{\omega}} \sin^2(\omega t) dt = \pi \varepsilon_0^2 \omega^2 \eta(\omega) \# (S11)$$

Equating Eq.(S9) and Eq.(S11) gives,

$$\eta(\omega) = \frac{E^{''}(\omega)}{\omega} \# (S12)$$

Thus, we can define an effective viscosity via Eq.(S14) using the loss modulus $E^{''}(\omega)$. In some literature, the viscosity defined in Eq. (S14) is also called the dynamic viscosity [3].

From Eqn S1, with $E_\infty = 0$, the modified power-law relaxation function becomes,

$$Y(t) = \frac{E_0}{\left(1 + \frac{t}{t_R}\right)^m} \# (S13)$$

The complex modulus associated with this relaxation function is,

$$E^*(\omega) = i\omega \int_0^\infty Y(t) e^{-i\omega t} dt = i\omega E_0 \int_0^\infty \left(1 + \frac{t}{t_R}\right)^{-m} e^{-i\omega t} dt = E_0 e^c c^m \Gamma(1 - m, c) \# (S14)$$

where $c = i\omega t_R$ and $\Gamma(s,c) = \int_c^\infty z^{s-1} e^{-z} dz$ is the upper incomplete gamma function.

An alternative equivalent expression using the Kummer's function $U(1,1-m,i\omega t_R) = \int_0^\infty \frac{e^{-i\omega t_R v}}{(1+v)^{m+1}} dv$ is,

$$E^*(\omega) = E_0\left[1 - \frac{m}{t_R}\int_0^\infty \frac{e^{-i\omega t}dt}{\left(1+\frac{t}{t_R}\right)^{m+1}}\right] = E_0\left[1 - mU\left(1,1-m,i\omega t_R\right)\right]\#(S15)$$

Therefore, the effective viscosity $\eta(\omega)$ normalized by instantaneous modulus E_0 is given by,

$$\frac{\eta(\omega)}{E_0} = \frac{Im\left[E^*(\omega)\right]}{E_0\omega} = \frac{Im\left[e^c c^m \Gamma(1-m,c)\right]}{\omega}, c = i\omega t_R\#(S16)$$

3. Conversion of measured spheroid diameter to height

Compression of a spheroid under large deformation does not yield simple analytical results. Therefore, we employed the finite element method (FEM) to investigate the conversion from the change in area ΔA to the change in height Δh. The definition of each parameter is shown in Fig. S4.

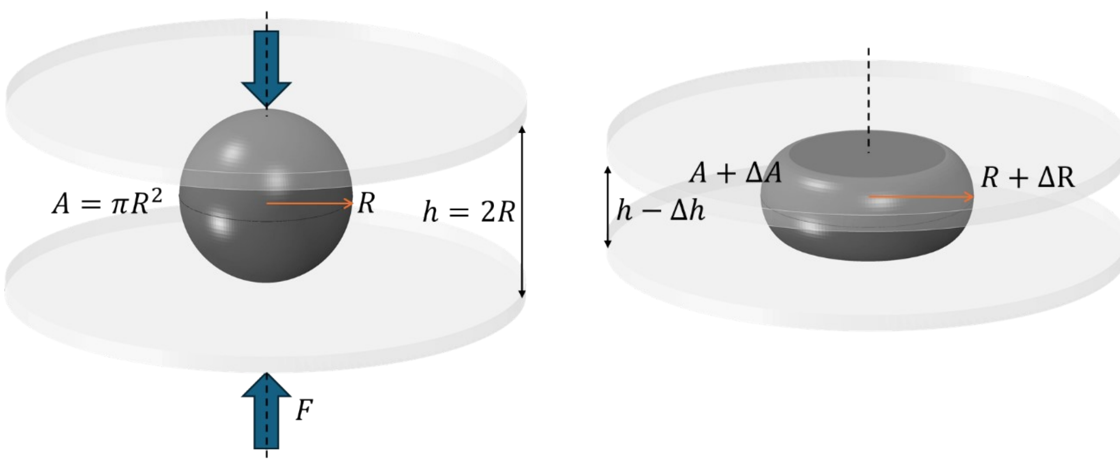

Figure S5: Illustration of a geometric relation of an initial stress-free (a, left) /compressed (b, right) sphere. Here, F is the force exerted onto the sphere, R is the radius of the sphere in the mid-z plane, A is the area of the sphere in the mid-z plane, and h is the height of the sphere. Left/right panel shows the sphere under initial stress-free/compressed state.

The simulation was conducted using Abaqus with axisymmetric hybrid elements (CAX4H). We assumed frictionless hard contact between the hyperelastic sphere and rigid plates and used an incompressible neo-Hookean material model for the spheroid.

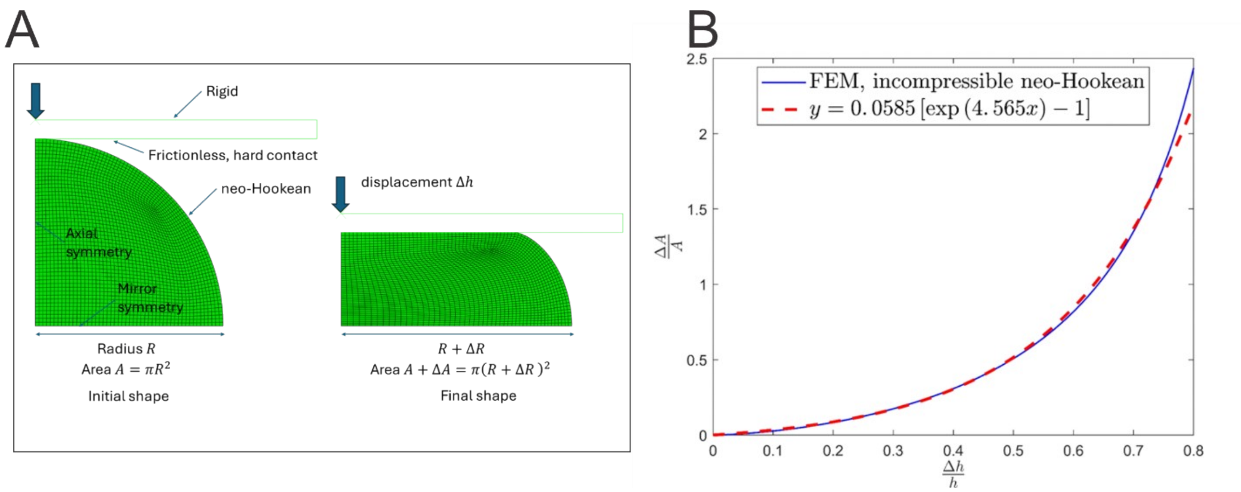

Figure S6: (A) FEM computation setup. Here, material property is assumed to be neo-Hookean, and the volume is conserved. **(B)** Relation of area change versus height change computed from the FEM calculation. This relationship is independent of the radius of sphere and the elastic modulus, here $x = \Delta h/h$.

Under these conditions, a normalized master curve between $\Delta A/A$ and $\Delta h/h$ can be obtained from the simulation results, which does not depend on the spheroid radius R and the Young's modulus E. Hence we conclude that this relation is purely geometry and is insensitive to the modulus.

We propose a simple exponential function to fit the FEM results:

$$\frac{\Delta A}{A} \cong 0.0585\left[e^{\left(4.564\frac{\Delta h}{h}\right)} - 1\right] \#(S17)$$

Although this relationship is derived in the compressed state, it is purely geometric in nature; thus, we use it as an approximation to analyze data in other states, such as during strain recovery stage after pressure release. The normalized strain $\bar{\varepsilon}(t)$ during strain recovery, $t > T^-$, is converted from the area change $\frac{\Delta A(t)}{A}$ using Eq.(S17). T^- is the time just before unloading.

$$\bar{\varepsilon}(t) = \frac{\Delta h(t)}{\Delta h(T^-)} \cong \frac{\ln\left[\frac{1}{0.0585}\frac{\Delta A(t)}{A} + 1\right]}{\ln\left[\frac{1}{0.0585}\frac{\Delta A(T^-)}{A} + 1\right]} \cong \frac{\ln\left[17.1\frac{\Delta A(t)}{A} + 1\right]}{\ln\left[17.1\frac{\Delta A(T^-)}{A} + 1\right]} \#(S18)$$

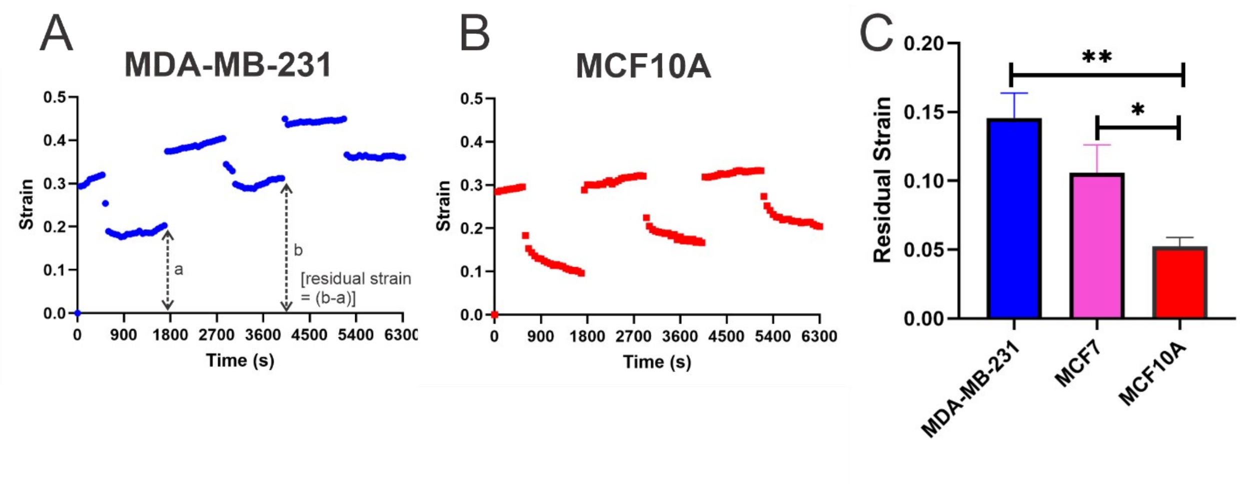

Figure S7: Residual strain calculated using the real strain values obtained via change in Area to change in height conversion discussed in S2. The stars were obtained using a nonparametric t-test (Mann–Whitney test with **: $P < 0.01$ and *: $P < 0.05$).

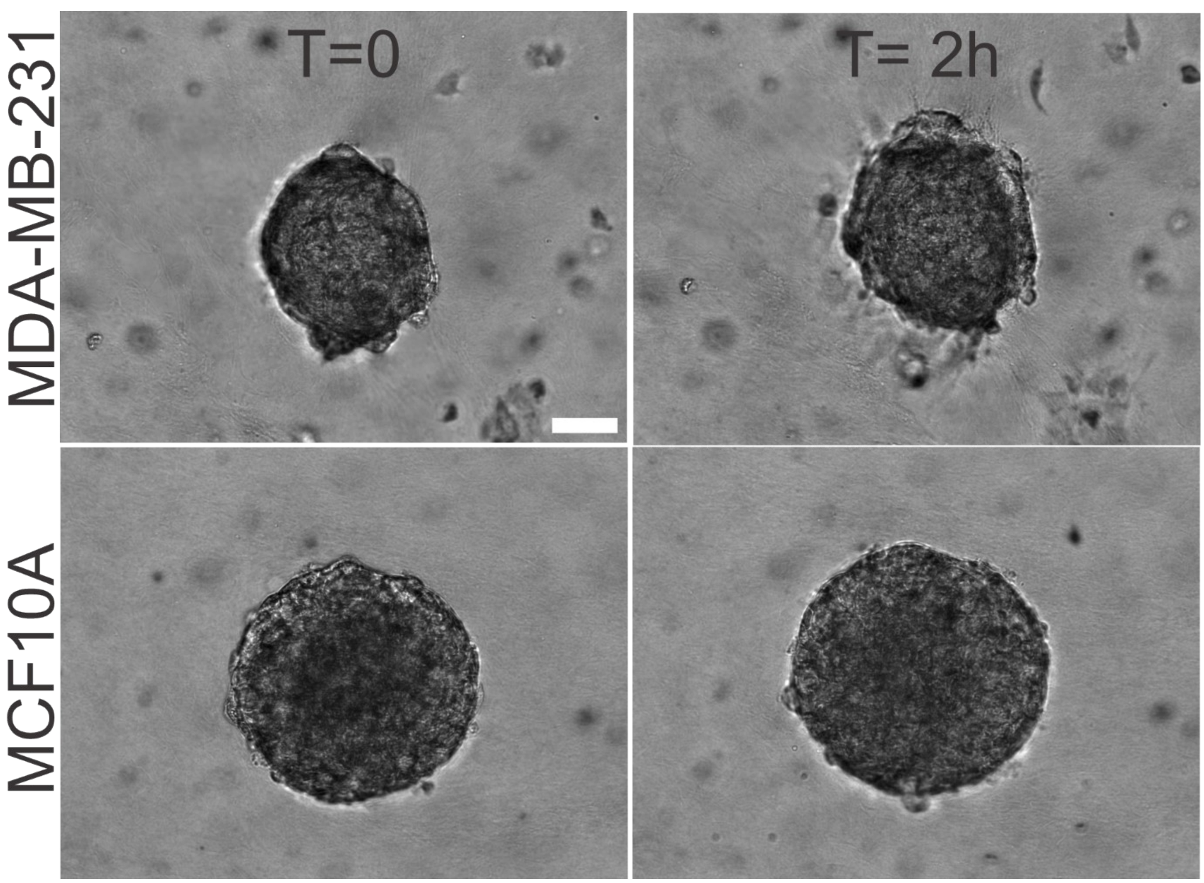

Figure S8: Malignant MDA-MB-231 spheroids begin to show protrusions indicating invasion at the end of three cyclic compressions. Malignant MDA-MB-231 and non-malignant MCF10A spheroids at the start and end of T = 40 min cyclic compression cycle. The scale bar is 50 µm.

Movies:

SMovie 1: Compression of an MDA-MB-231 spheroid under 14 kPa, T = 40 sec square wave pressure input. This movie illustrates the spheroid deformation dynamics during short time scales cyclic loading for malignant tumor spheroid.

SMovie 2: Compression of an MCF10A spheroid under 14 kPa, T = 40 sec square wave pressure input. This movie illustrates the spheroid deformation dynamics during short time scales cyclic loading for healthy epithelial breast spheroid.

SMovie 3: Compression of an MDA-MB-231 spheroid under 14 kPa, T = 40 min square wave pressure input. This movie illustrates the spheroid deformation dynamics during long time scales cyclic loading for malignant tumor spheroid.

SMovie 4: Compression of an MCF10A spheroid under 14 kPa, T = 40 min square wave pressure input. This movie illustrates the spheroid deformation dynamics during long time scales cyclic loading for healthy epithelial breast spheroid.

SMovie 5: COMSOL finite element simulation of PDMS piston hat compressing the tumor spheroids. PDMS was modeled as a linear elastic material with modulus of 1.33 MPa and Poisson's ratio of 0.49, while the tumor spheroid was modeled as incompressible Neo-Hookean hyperelastic materials.

References:

(1) Bagley, R. L. Power law and fractional calculus model of viscoelasticity. *AIAA journal* **1989**, *27* (10), 1412-1417.
(2) Christensen, R. M. *Theory of viscoelasticity*; Courier Corporation, 2013.
(3) Vincent, J. Structural biomaterials. In *Structural Biomaterials*, Princeton University Press, 2012.